Research article

Molecular network mechanism in cerebral ischemia-reperfusion rats treated with human urine stem cells

Lang-Chun Zhang [a,b,1], Na Li [b,1], Ji-Lin Chen [b], Jie Sun [b], Min Xu [b], Wen-Qiang Liu [c], Zhong-Fu Zuo [d], Lan-Lan Shi [a], Ting-Hua Wang [a,*], Xiang-Yin Luo [a,**]

[a] Department of Neurosurgery, Xiang Ya Hospital of Central South University, Changsha, 410078, China
[b] Animal Canter Department of Anatomy, Kunming Medical University, Kunming, 650500, China
[c] College of Basic Medicine, Jinzhou Medical University, Jinzhou, 121000, China
[d] Department of Anatomy, Jinzhou Medical University, Jinzhou, China

ABSTRACT

Objective: To explore the effect of human urine-derived stem cells (husc) in improving the neurological function of rats with cerebral ischemia-reperfusion (CIR), and report new molecular network by bioinformatics, combined with experiment validation.
Methods: After CIR model was established, and husc were transplanted into the lateral ventricle of rats , neurological severe score (NSS) andgene network analysis were performed. Firstly, we input the keywords "Cerebral reperfusion" and "human urine stem cells" into Genecard database and merged data with findings from PubMed so as to get their targets genes, and downloaded them to make Venny intersection plot. Then, Gene ontology (GO) analysis, kyoto encyclopedia of genes and genomes (KEGG) pathway analysis and protein-protein interaction (PPI) were performed to construct molecular network of core genes. Lastly, the expressional level of core genes was validated via quantitative real-time polymerase chain reaction (qRT-PCR), and localized by immunofluorescence.
Results: Compared with the Sham group, the neurological function of CIR rats was significantly improved after the injection of husc into the lateral ventricle; at 14 days, P = 0.028, which was statistically significant. There were 258 overlapping genes between CIR and husc, and integrated with 252 genes screened from PubMed and CNKI. GO enrichment analysis were mainly involved neutrophil degranulation, neutrophil activation in immune response and platelet positive regulation of degranulation, Hemostasis, blood coagulation, coagulation, etc. KEGG pathway analysis was mainly involved in complement and coagulation cascades, ECM-receptor. Hub genes screened by Cytoscape consist ofCD44, ACTB, FN1, ITGB1, PLG, CASP3, ALB, HSP90AA1, EGF, GAPDH. Lastly, qRT-PCR results showed statistic significance (P < 0.05) in ALB, CD44 and EGF before and after treatment, and EGF immunostaining was localized in neuron of cortex.
Conclusion: husc transplantation showed a positive effect in improving neural function of CIR rats, and underlying mechanism is involved in CD44, ALB, and EGF network.

1. Introduction

Cerebral ischemia (CI) has been well-known as one of the main causes of morbidity and mortality in the world, in which. Ischemic stroke will lead to neuronal damage while cerebral ischemia reperfusion (CIR) will aggravate the functional injury process [1], and effective therapy is missing, especially 4 h after CIR [2,3]. Not only can CIR lead to learning and memory impairment, neurological dysfunction and brain death, but also is associated with morbidity, mortality and disability, and the underlying mechanism is involving in inflammatory reaction (Hu, Y et al., 2019). Thrombolytic therapy is the standard treatment for ischemic stroke. However, reperfusion to restore cerebral blood flow in ischemic brain tissue eventually leads to irreversible brain damage, in which, a variety of complex molecular mechanisms, including excessive oxidative stress and inflammatory response, calcium overload and apoptotic cell death, are involved in the progression of ischemic injury.

Cell therapy is an effective strategy for the treatment of severe neurological diseases, especially ischemic stroke. It has been known that bone mesenchymal stromal cells (BMSC) transplantation is an effective strategy for the clinical treatment of ischemic stroke, and its benefits have been confirmed [4]. Definitely, BMSC can be used to repair or inhibit neurodegeneration by inhibiting cell death and secretion of a series of growth factors as well as anti-inflammatory cytokines in ischemic brain tissue [5]. In addition, a number of clinical studies have shown that (NSC) transplantation is an effective method to treat ischemic stroke through various mechanisms, such as protecting the blood-brain barrier (BBB), alleviating neuroinflammation in the brain, enhancing neurogenesis and angiogenesis, and achieving functional neurological recovery [6]. Additionally, NSC have been used in some experimental studies and preclinical trials, but invasive medical procedures to harvest NSC or MSC may present potential complications, serious ones may endanger the life of the donor. The ideal source of stem cells would be less harmful to the donor and easier to collect and expand in large numbers.

Human-derived urine (husc) can be collected easily without health risks throughout the patient's life cycle, they can even be collected daily [7]. These cells can effectively be induced as ectoderm and mesoderm and endoderm lineages [8]. The ectodermal neural lineage was obtained by adding basic fibroblast growth factor (bFGF) to neural induction medium, and about 40% of the induced cells expressed some neural markers and showed neurogenic extension and processes in vitro and in vivo [9]. Even though a few cells have a "rice-like" shape in urine, they can continuously multiply to more than 20 generations with a multiplication rate of more than 60. Currently, husc could be isolated from fresh urine and propagated in a simple, non-invasive and low-cost procedure [10,11], and also have differentiation potential and paracrine action [12]. However, no report to confirm the effect of husc in ischemic stroke model.

In this study, we used animal experiments to verify that transplantation effect of husc to improve the neural function in CIR rats, and using bioinformatics methods [13,14], to uncover the underlying molecular network mechanism.

2. Materials and methods

2.1. Culture and amplification of husc

A sterile urine sample approximately 300 ml was acquired from urine of health adult female, followed by a centrifugation at 1500 rpm for 10min, then the supernatant was gently poured out in the biosafety cabinet, and remaining 0.5 ml urine at the bottom was collected, washed again by urine cell cleaning. This was followed by an inoculation, at culture flask, and regular observation till and clone formation. Next, husc were cultured up to 3 passages, to amplify the number of urine stem cells, then identified by using immunofluorescence staining by specific marker.

During passage, the cells were re-suspended in a 15 ml centrifuge tube and centrifuged at 1500 rpm for 5min, then the supernatant was discarded and 1 ml urine stem cell special medium was added for re-suspension. Next, 80 μl urine special medium mixed with +10 μl 0.4% Trypan blue dye were added into 10 μl cell suspension for counting cell number in the cell counting apparatus, till the result display.

2.2. Animal model and husc administration

SD rats were purchased from Experimental Animal Center of Kunming Medical University, the production license number is SCXK (Yunnan) K2020-0004. To perform the experiment, all rats were divided into sham group(n = 7), CIR group (n = 10), and husc treated group(n = 6), with ethic number KMMU20220891. Before operation, the rats were fasted for 8–10 h, then anesthetized with 3% sodium pentobarbital. Subsequently, the common carotid artery, external carotid artery and internal carotid artery on the right side were separated and exposed again by the method of thread embolization. The thread plug was inserted into the internal carotid artery with depth 18 mm, and the thin wire at the distal end of CCA was tightly fastened. Then the wound was closed, and the tether was taken out 1 h later. To perform husc transplantatioin, a craniotomy was performed in the right lateral ventricle of the rats, coated 1.5 mm beside the sagittal line and 2 mm backward. Then,10 μl stem cells(1×10^5) were injected into lateral ventricle with stereolocator and microinjector. Lastly, the hole was sealed with bone wax after the injection [15].

2.3. Modified neurological severity scale (mNSS) assessment

The three groups of rats were evaluated for neurological severity on 1d,3d,5d,7d,10d and14d. There are 5 items in total: 1. Rat tail about 1 m away from the point (0–3 score); 2. Motor function observation (0~3score); 3. Beam experiment (0–6 score); 4. Sensory

function (0–2 score); 5. Reflex activity (0–4 score). Three people with blind will score at the same time, and the final results will be taken as the average score of three people for statistics.

2.4. TTC staining

Brain samples were cut into 2 mm thick sections. The sections were stained with 2,3,5-triphenyltetrazolium chloride TTC (2%) at 37 °C for 0.5 h and fixed with 4% paraformaldehyde at 4 °C overnight. Sections were photographed and the size of cerebral infarction was measured and analyzed with Image J.

2.5. Query CIR and hub gene targets

When open browser, we entered Genecards from Baidu. By using website (https://www. Genecards.org), we typed into "Cerebral reperfusion" and "Human urine stem" on Genecards database to search respective target gent and download the gene targets in Excel format. In Genecards database, the higher the Relevance score was, the more closely the target was, then they were preserved.

2.6. Venny diagram analysis of both CIR and husc

Venny intersection diagram was performed between CIR and husc, so as to obtain the intersection genes. Using Venny2.1 (https://bioinfogp.cnb.csic.es/tools/venny/),we entered respective target gene both CIR and husc, in List1 and List2, then acquired their cross genes, and changed their styles color, and downloaded images.

2.7. Integrate analysis with the genes from PubMed

Key words "Cerebral ischemia reperfusion", and "Stem cell transplantation" were input so as to collect the latest findings that do not present in Genecards. Then we merged them into cross gene from Venny analysis.

2.8. GO and KEGG analysis

GO analysis, as an international standardized functional classification system of gene, provides dynamically updated control terms and strictly defined concepts to comprehensively describe the characteristics of genes and their products in any organism. GO enrichment analysis provided all of the GO terms, which were significantly enriched in target genes compared to the genomic background and filtered corresponding biofunctional target genes. In this study, all targets were mapped to the gene ontology database (http://www.geneontology). The number of genes per semester, and path-based analysis was used to characterize the biological function of the target, moreover, Pathway enrichment analysis was performed by using the application of KEGG pathways database (http://www.genome.jp/kegg/) to discover the important signal transduction pathways. To reach this aim, R software version 3.6.0 (http://www.r-project.org)was installed in the Java environment, and rSQLite, Cluster Profiler, and org are also required. Related, and Dose, enrich Plot, GGplot2, colorspace, stringi, pathView, are needed. Then all gene list was copied and pasted into the R software window for so and KEGG analysis. After enrichment analysis of GO and KEGG, histogram, bubble diagram and signal pathway diagram were plotted using dB, enrichment diagram and GGplot2, respectively.

2.9. PPI protein interaction

By using string Database (https://string-db.org/), 252 common genes were linked in string database and set biological species to "Homo" in the option of "organization", then make protein interaction map, and export its high-definition interaction map (400PPI) and interaction relationship table. Meanwhile, hub genes were screened according to Degree value in Cytoscape, and 10 hub genes were noticed.

Table 1
Primers for Real-Time polymerase chain reaction.

Gene	Sense primer	Anti-sense primer
ACTB	CCTCACTGTCCACCTTCCA	GGGTGTAAAACGCAGCTCA
ALB	CGTCAGAGGATGAAGTGCT	TGGTGAGGTCTGTTGCC
CASP3	TGGACAACAACGAAACCTC	ACACAAGCCCATTTCAGG
CD44	GTACATCAGTCACAGACCT	CTGCTGACATCCTCATCTAT
FN1	ATTCTGTAGGCCGTTGGA	TACTGCTGGATGCTGATGA
ITGB1	CGTGCGGAAGACAAGTG	CTCACAATGGCACACAGG
PLG	GCCCAACCTACCAATGTCT	AGTTTTCTGGCGTCCTGTT
EGF	GTAGTGGTGGCCCTTGG	GCTGGGTGTGAGAGGTTC
GAPDH	TCTTTGCTTGGGTGGGT	TGGGTCTGGCATTGTTCT
HSP90AA1	TTTGGTGCCTGACTTGG	TAAACTGGACTCGGGGAA

2.10. Quantificational real-time polymerase chain reaction (qRT-PCR) validation

To validate the core genes, the penumbra of brain tissues from each rat in respective group was harvested, then total RNA was extracted using Trizol, and cDNA was synthesized according to the reagent kit instructions. When the OD 260/OD 280 ratio of the extracted RNA samples ranged from 1.8 to 2.0, qRT-PCR was performed. The primer sequences are shown in Table 1. The reaction conditions were as follows: initial denaturation at 95 °C for 5 min, followed by 40 cycles of denaturation at 95 °C for 10s, and annealing and extension at 72 °C for 45 s. The relative expression of target genes was assessed using the $2^{-\Delta\Delta Ct}$ method (Table 1) .

2.11. Immunofluorescent staining

The husc were harvested and performed immunofluorescence. After washed with $1\times$ Phosphate-Buffered Saline, 0.1% Tween® 20 Detergent (PBST) (Batch no. P1003, SolarbioCat, China) solution was used for 5×5 min, and 5% sheep serum was used as a sealer, while 0.3% Triton solution (Batch no. EZ6789D142, Biofroxx) was designated as a cell permeabilizer to punch holes in the membrane. After standing at room temperature for 3 h, the cells were incubated with primary antibody (CD44, 1; 200, mouse, Boaishen; CD45, 1; 300, mouse, Boaoshen; CD90, 1:200, mouse) at 4 °C overnight, and they were continuously washed 5 times with PBST for 5 min each, followed by an incubated with fluorescent dye-labeled secondary antibody (488, anti-mouse, 1:200; cy3, anti-mouse, 1:200) at 37 °C for 1 h, and washed 5 times with PBST for 5 min each. Subsequently the cells were restained with DAPI and the expression of CD44, CD45, CD90 was observed by fluorescence microscope.

2.12. Statistical analysis

SPSS software was used for statistical analysis and graphing. A one-way ANOVA with post hoc Tukey's test was used for comparing multiple groups. Measurement data in each group are presented as a mean ± S.E.M (standard error of mean). $P \leq 0.05$ was considered statistically significant. Graph was generated using Prism 6 (GraphPad).

3. Results

We identified the cultured husc by specific marker and found they expressed CD44 and CD90, but not CD45, which was consistent with the stem cell characteristics of husc in literature. Then the cell viability of husc was tested, and the data were as shown in Table 1 and Fig. 2. Morphologically, on day 2, day 4 and day 6, as well as the P3 generation cells were observed after the resuscitation of different urine cells. The husc were mainly adherent with spindle shaped, together with round, diamond, spindle and polygon partly (spherical, spindle, triangular) with the growth at day 6 in third passage (Figs. 1–3, Table 2).
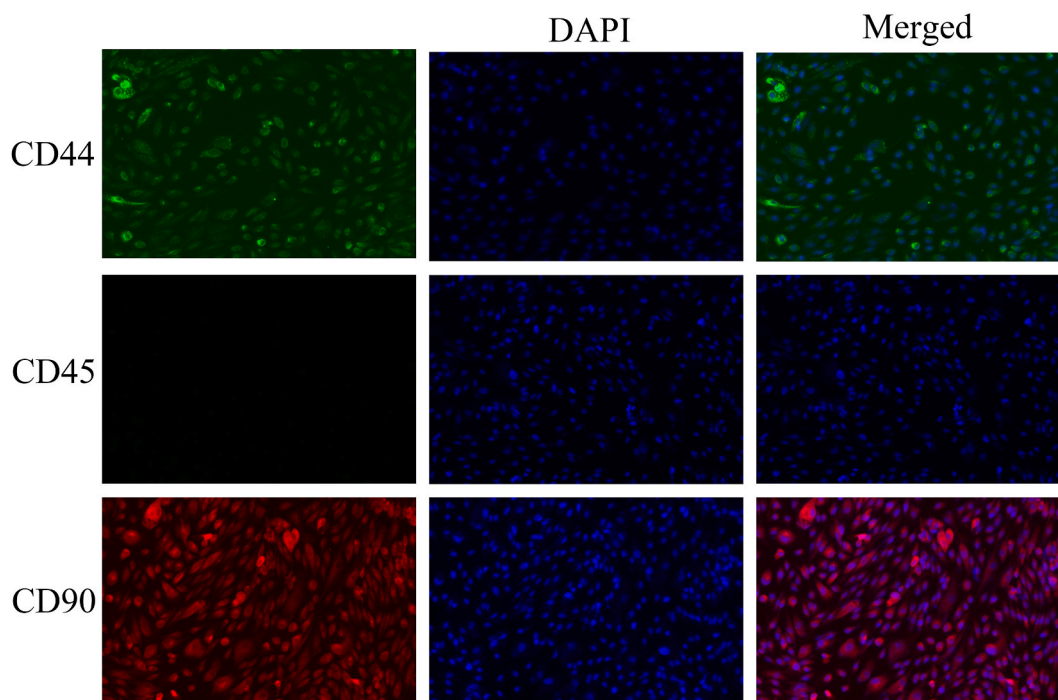

Fig. 1. Identification of human urine stem cells.

3.1. Behavioral data indicated by mNSS score

In order to verify the success of modeling, mNSS neurobehavioral evaluation was performed in each group at 1, 3, 5, 7, 10 and 14 days after surgery, respectively. SPSS was used for analysis, univariate measurement ANOVA was used for statistics and mapping, compared with the sham group, the neurological function in CIR rats was significant increase. Moreover, after injection of husc into the lateral ventricle, the neurological function was lower than that of CIR, which was statistically significant at day 14, and sphericity test and Greenhouse-Geisler was used, also. The data did not meet the sphericity hypothesis. Referring to the correction results of Greenhouse-Geisler, the results showed that both time and time*group had P < 0.05, suggesting differences in each time indicator variable,and the effect of treatment factors on index variables will change with the time. The comparison between groups and the test of inter-subject effect gives ANOVA of the treatment factor groups. P < 0.005 indicated that there was a difference in the amount of difference between different treatment groups. In addition, TTC stain confirmed the brain infarct was apparent increase, while it decreased significantly in the treatment of husc (Fig. 4A and B)

The effect of husc transplantation into cerebral ischemia-reperfusion was verified by bioassay. A total of 1493 genes were detected in Genecars for CIR. Some genes are shown in Table 3.

A total of 1095 genes of human urine stem cells were found in Genecars. Some genes are shown in Table 4.

3.2. Venny diagram

The gene crossover between CIR and husc was analyzed, in which, 258 key targets of Venny diagram were obtained by deleting duplicates, as shown in Fig. 5.

3.3. Cross genes were integrated with data from PubMed

For input key words CIR and husc in PubMed, respectively, Genes reported and unreported in crossest were screened and sorted into Excel tables. There are 258 intersection targets in the Venny diagram, among which, 6 genes have been reported and 252 genes have not been reported in PubMed, shown in Tables 5–7,8.

3.4. The GO analysis

We analyzed the mechanism of husc to improve CIR. The top 10 biological processes (BP) involved in GO enrichment analysis are as follows: Neutrophil activation involved in immune response, neutrophil degranulation, Hemostasis, blood coagulation, negative regulation of coagulation, regulation of coagulation endopeptidase, and activity regulation of Peptidase activity. The top 10 factors involved in cell component (CC) in GO enrichment analysis were: Vesicle Lumen, Cytoplasmic Vesicle Lumen, Secretory Granule Lumen, Collagen −containing extracellular matrix, blood Microparticle, vacuolar Lumen, platelet alpha granule lumen, platelet alpha granule, endoplasmic reticulum Lumen, Ficolin −1− Rich Granule. The top 10 factors involved in molecular function (MF) in GO enrichment analysis were enzyme inhibitor activity, Endopeptidase inhibitor activity and Peptidase regulator Activity, Peptidase inhibitor activity Endopeptidase regulator activity, Sulfur compound binding, Glycosaminoglycan binding, Antioxidant activity, Heparin Binding, Extracellular matrix structural constituent and Protease binding, shown in Fig. 6. Fig. 6 shows that BP participates in many biological processes, among which, neutrophil degranulation is the most abundant biological process. Neutrophil activation involved in immune response, and platelet degranulation. These biological processes constitute an important part of cell development. CC involves many cellular components, among which Vesicle Lumen is the most important chemical component, followed by Cytoplasmic Vesicle Lumen and Secretory granule Lumen, which constitute cellular components related to cell development. MF involves many molecular characteristics, among which enzyme inhibitor activity is one of the most important, followed by endopeptidase inhibitor activity, Peptidase regulator activity, these molecules constitute molecular functions related to cell development (Fig. 6A–C).
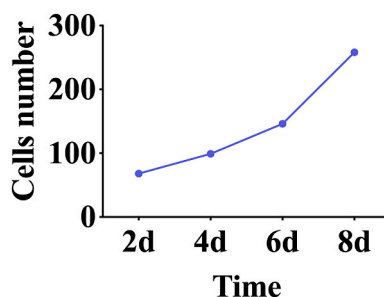

Fig. 2. Cell viability test curve.
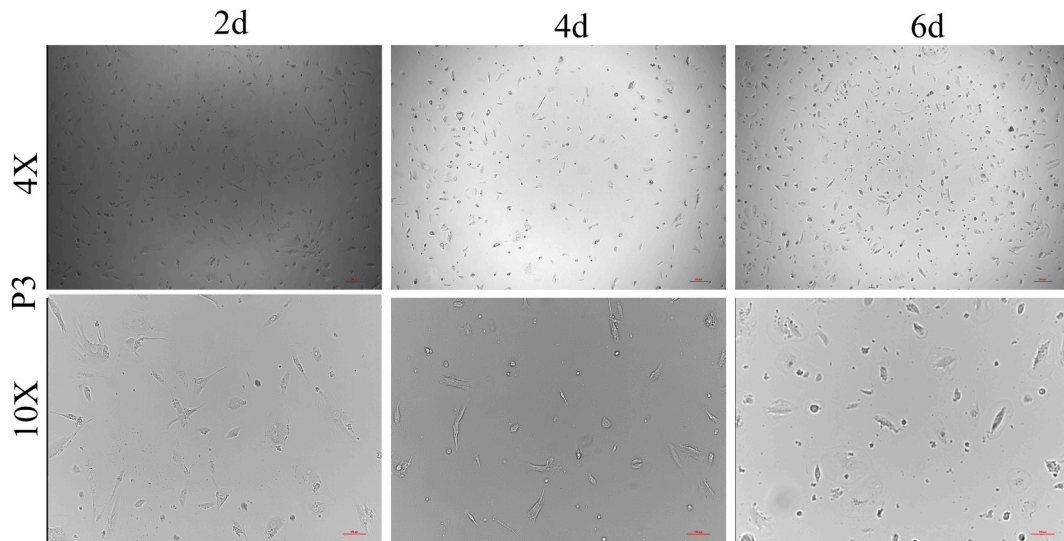
Fig. 3. Bright field images of different urine cells after resuscitation at 40 and 100 times.

Table 2
Cell viability test results.

Cell viability test results	
Total cell concentration	7.18E+05
Living cell concentration	6.96E+04
Dead cell concentration	2.22E+04
Live cell rate	96.91%
Mean cell size	14.19um
The dilution ratio	2
Cell agglomeration rate	2.105%
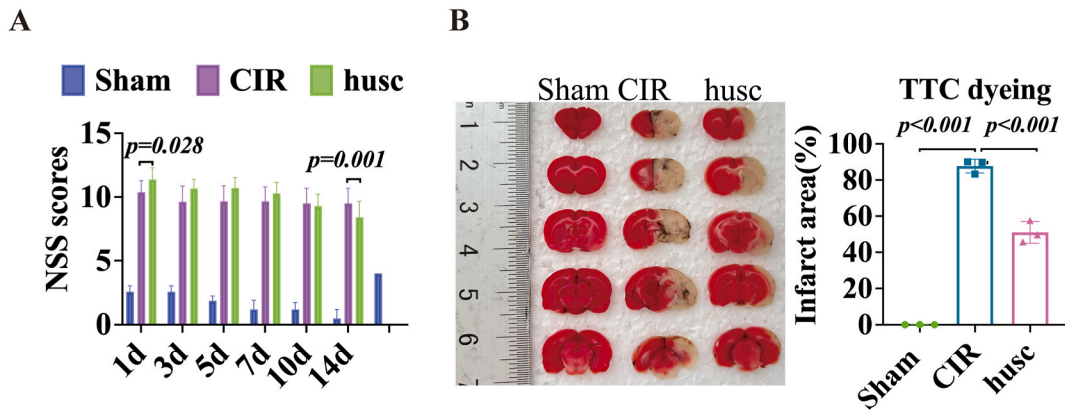
Fig. 4. Effect of CIR and husc treatment. A showed neural behavor. B–C showed TTC staining and quantitative analysis.

3.5. KEGG pathway analysis

To elucidate the mechanism of husc in CIR, we analyzed the KEGG pathway after gene crossover (Fig. 7). The results showed that the top 10 pathways in KEGG pathway were: Complement and coagulation cascades, ECM-receptor interaction, Glutathione metabolism, Proteoglycans in Cancer, Legionellosis, Lipid and atherosclerosis, Staphylococcus aureus infection, Amoebiasis, Fluid shear stress and atherosclerosis.

Table 3
Repeat measure ANOVA table.

Repeat measure ANOVA table					
Variables	DF	SS	MF	F	P
Intervene	2	2306.271	1153.136	233.912	< 0.001
Intergroup error	20	98.596	4.930		
Time	2.943	141.833	48.193	91.143	< 0.001
Time*Intervene	5.886	32.503	5.522	10.443	< 0.001
Repeated measurement	58.861	31.123	0.529		

Note: DF is the degree of freedom, SS is the sum of squares, MF is the mean square and P is the significance P-value.

Table 4
Some gene targets of CIR.

APP	CBS	KCNJ5	CASP1	NTRK2	TSPO	ARID1B	F8
KRIT1	SLC1A2	ADM	F13A1	CTSD	HTRA2	LPL	IGFBP3
CST3	HMOX1	ODC1	ATP1A2	ITPR1	SLC9A1	EDNRA	IL12A
F2	MMP9	CYCS	AIFM1	FGB	GPT	EDNRB	CCL3
IL6	SELE	PDGFB	ANGPT1	HGF	SLC6A4	SMAD4	CCL5
TNF	EPO	NFE2L2	APOB	TLR2	CSF1R	RELA	HSPB6
NOS3	SELP	MAP2	PARP1	FOS	PF4	TGFBR1	AIF1
COL4A1	S100B	NPPA	FAS	HSPA8	PTGS1	ADA	CHAT
ACE	SOD2	TEK	CSF3	MIR146A	PRKCE	MIR155	OCLN
F5	JAK2	TSC2	HSPA1A	PPARG	PRKAA2	ACTB	CTSL
NOS2	MIR21	CASP9	AQP4	GLUL	TOMM40	DRD2	HMGCR
ENG	SERPINE1	GJA1	SLC6A3	CD40LG	MIR34A	TIMP3	PARK7
SOD1	CXCL8	FLT1	SPTAN1	DLG4	PDP1	MIR145	SPP1
MTHFR	THBD	PON1	G6PD	EPRS1	REN	PIK3CG	MCU
ICAM1	CAT	HSPA5	VCAM1	NPY	PTK2B	CDKN2A	ACTG1
PIK3CA	VWF	AKT1	LTA	SLC1A1	HP	PPARA	CACNA1B
MPO	HSPA4	SHH	MPL	MIR210	SELL	NLRP3	ABCB1
GAD1	ALB	SNCA	CR1	LMNA	ADORA3	CDON	MIR126
TP53	MB	GRIN1	ACHE	PECAM1	TNFRSF1A	AGER	AVP
VEGFA	GRIN2B	AGTR1	ADORA1	ATM	IL17A	FN1	PRKN
PTEN	TGFB2	MAPK14	CALR	ANGPT2	SYNGAP1	MYH7	MUC1
IL10	MMP2	IL18	ELANE	TIMP1	MME	CD40	SERPINA1
MEF2C	IGF1	YRDC	TXN	LOX	NGB	CNR1	CKB
CASP3	ENO2	MTOR	JUN	FLNA	HTR2A	TTN	ADCYAP1
PLAT	NPPB	SMARCAL1	CTLA4	SLC8A1	THBS1	STAT3	CPT2
SMARCA4	F3	PLG	CP	ERCC2	TGIF1	TNNI3	COMT
MAPT	IL1RN	ADAMTS13	EGF	ANXA5	GDNF	MIF	ITGA2B
GFAP	ACTA2	SLC2A1	ADRB2	ITGAM	LAMB1	TNNT2	ADRB1
EDN1	SETD2	APOH	IDH1	CTSB	HSPG2	PCNA	OLR1
PSEN1	SERPINA3	PROC	LDLR	PLAU	MT-CO1	MBP	BGN
SERPINC1	PLA2G6	EGR1	APOA1	NES	RPS27A	NFKB1	FMR1
TLR4	KDR	IFNG	HSPB1	SLC12A2	ADIPOQ	XIAP	NOL3
HIF1A	PTGS2	VLDLR	ALOX5	SMAD2	IL1A	IL13	ENTPD1
PRNP	BAX	INS	SLC17A5	EGFR	NCF1	KCNMA1	SIRT1
CTNNB1	KNG1	AGT	PROCR	LEP	CDKN3	ABCA1	SRC
IL1B	SERPINI1	GRIN2A	THPO	NOTCH1	SH2B3	ITGB2	GLO1
COL3A1	CXCL12	ITGB3	PSAP	BAD	GAPDH	PLA2G7	CA2
CRP	GRIK2	HMGB1	FGA	STAT1	VCP	MAPK8IP1	ABCC8
COL4A2	GP1BA	CALCA	CLU	IL2	AOC3	ITGB1	PRKG1
BCL2	PIK3C2A	FGF2	NGF	BCL2L1	SST	CAMK2A	TIE1
BDNF	GSR	IL4	MAPK8	ESR1	GSS	TERT	CFLAR
XDH	CD36	ADORA2A	TIMP2	IKBKG	FGFR2	BMP6	PDE5A
NOS1	CDK5	MAPK1	MBL2	SMPD1	SDHB	DNM1L	MLC1

3.6. PPI protein network construction

252 intersecting genes not reported in Table 5 were selected to performed String (https://string-db.org/). After UniProt Transformation, protein interaction network analysis can understand intermolecular interactions and protein interaction network diagrams. As shown in Fig. 8, Each node represents a protein target, and each connector represents the interaction between two target proteins. The larger the node, the higher the centrality of the protein target, the thicker the connecting line, and the stronger the interaction between the two proteins. Especially, it can be seen that there are many histones and there are complex relationships among genes, which is mainly in a circular concentrated in the middle of the protein. In addition, there is a protein relationship formed at the upper
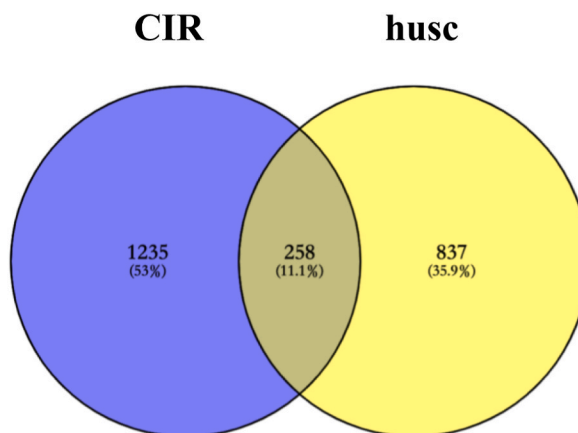
Fig. 5. Venny diagram between CIR and husc. The left circle is the target gene from CIR, the right circle is the target gene from husc and the intersection target between them was acquire in the middle.

Table 5
Partial gene targets of husc.

IL6	MUC4	UBA1	ACO1	NPHP3	EEF1G	SPPL2A	PROM2
KRAS	IGFBP2	PPT1	MGAT5	CDH16	DDAH1	CAPN7	FUCA2
TERT	C3	LAMP1	GNB3	PPT2	NID2	IST1	SECTM1
BRAF	NEU1	IRAK1	SERPINB9	LBP	LTBP2	KRT75	MYL6B
CD44	ANXA2	DMBT1	AQP2	CCT4	ANXA3	TUBB8	PEF1
CXCL12	TXN	TPI1	ACTR2	ACTN3	ATP6V1A	PYGB	STK25
FGFR3	YWHAE	NECTIN2	DKK3	CFD	H4C12	SERPINA6	H2AC16
ITGB1	STXBP2	MYH10	GPI	UMOD	COTL1	ARHGAP1	EHD4
CDH1	PLA2G2A	KL	SDCBP	EPX	STK26	MGAT1	LRRC57
FGF2	MMP7	HNRNPK	APRT	BAIAP2L1	UPK1A	CLEC3B	GATM
IL1B	SERPINA1	MTHFD1	ARF1	C8B	CFB	GNG4	C8A
CASP8	LGALS1	ARSB	FAT4	NPHS2	CA1	RAB21	MAN1C1
EGF	TUBB	H4-16	HNRNPM	SERPINF2	CACNA2D1	FIGNL1	DOP1B
FASLG	DNASE1	RDX	CETP	SLC12A1	NIBAN1	RAB11B	VPS25
MIR21	APOB	COL18A1	FGB	GSTM3	PYGM	TBC1D10A	GMPPA
CASP3	AQP1	CFL1	HMCN1	VPS4B	UGP2	SMS	PSMA8
PPARG	IGF2R	GP1BA	APOH	TUBB6	TXNDC5	PLPP1	H2AC17
ENG	FCGR3B	ARF6	CKB	FSHB	CAND1	ENO3	NUCB1
VCAM1	KLK3	PGK1	ENPEP	ATP5F1B	SERPINB8	ATP6V1B1	RAB5B
PROM1	KNG1	IGHG1	RBP4	SDCBP2	PACSIN3	NAPRT	PGM2
ABCB1	DMD	GAS6	FABP5	APOA2	PSMB2	ANXA7	GPD1L
HBB	CP	HSP90AB1	EFNB1	MACROH2A1	WASF3	CPVL	TNXA
FN1	PTPRJ	ACTG2	CSTB	MYOF	BASP1	COL15A1	PTTG1IP
CD36	CLTC	MB	LAMB2	SERPIND1	SERPING1	ACTR1A	ENTPD2
THY1	RPS27A	TLN1	GLO1	NIBAN2	GPLD1	LAP3	SPR
MMP9	KRT13	C5	HSPA1B	HPN	GLG1	FAM3C	MYO5C
EPCAM	TTR	LRP2	BST1	SFRP4	MYO1D	ATP6V0D1	H2AC6
MUC1	ACP1	CANX	GPX3	HRG	UPK3A	GCA	RNASE2
NF1	HBA2	YWHAZ	PRDX6	SELENOP	APCS	ARF3	ALDH1L2
ALB	RAB27A	LAMA5	MYO1C	ALDH9A1	ADH5	VPS4A	GUCA2B
RAC1	PRKACA	DAG1	AHCY	LILRB4	SUSD2	MXRA8	PPIC
MMP2	GSN	FGA	PIGR	GM2A	BTD	SULT2B1	H2AC13
SOD1	LAMA3	CNP	ALOX15B	GC	H2AZ1	AKR1C4	PLBD2
ANPEP	RXRA	IGFBP7	HPR	CST6	SORD	PROZ	MON2
SPP1	CFH	CD177	CLIC1	C1R	PAICS	QDPR	CTSZ
LHCGR	PODXL	CDH11	UBA52	MDH1	PAM	MLPH	NAAA
B2M	PRDX1	GGT1	AKR1C3	RHOG	H4C2	ACP2	CUTA
EDN1	KRT1	IGHM	ANO6	FBLN5	LTA4H	LUM	GSTT2
NT5E	PLG	COL4A2	PGM1	DSC1	MPI	H2AC4	CNDP2
SMO	ANXA1	CHI3L1	NID1	ARPC3	SERPINI1	DNPH1	XPNPEP1
ACTB	SERPINF1	CST3	FUCA1	PSME2	NPEPPS	AKR7A2	ATRN
CASP9	KRT20	CHL1	PSMA7	TUBB4B	H2AC20	CPNE2	ABHD14B
FCGR3A	SFN	PABPC1	GANAB	ACLY	SPON2	AOC1	BDH2

Table 6
Cross gene between CIR and husc.

CST3	ENO2	TXN	PLAU	ABCB1	GOT2	CDC42
F2	ACTA2	CP	SMPD1	MUC1	TF	LTF
IL6	SERPINA3	EGF	HP	SERPINA1	C4A	ITGAV
ACE	KNG1	IDH1	MME	CKB	ACTC1	EPX
ENG	SERPINI1	APOA1	THBS1	COMT	SERPINF2	FABP1
SOD1	CXCL12	HSPB1	HSPG2	BGN	LRP2	PRDX1
MPO	GP1BA	PROCR	RPS27A	GLO1	FASLG	GGT1
CASP3	GSR	PSAP	GAPDH	SOD3	CTSG	SERPINA4
EDN1	CD36	FGA	VCP	AQP1	NT5E	CD55
SERPINC1	CASP9	CLU	GSS	PROS1	HSP90AA1	SERPINF1
IL1B	PON1	CTSD	ACTB	PLA2G2A	GDF15	TKT
COL4A2	PLG	FGB	FN1	COL18A1	RETN	NID1
MMP9	APOH	HSPA8	MIF	AKR1B1	LGALS3	AHSG
SOD2	AGT	MIR146A	ITGB1	RAC1	ACE2	PTGDS
MIR21	FGF2	PPARG	TERT	LCN2	NAXE	GNA11
CAT	APOB	TIMP1	FABP3	C3	PNP	CD14
ALB	HSPA1A	FLNA	CTSL	NAGLU	SLC9A3R2	CHI3L1
MB	G6PD	ANXA5	PARK7	CASP8	ACP1	C5
MMP2	VCAM1	ITGAM	SPP1	CFH	KL	ALDH9A1
ELANE	CR1	CTSB	ACTG1	IGFBP2	CD44	AOC1
KRT18	GUSB	AXL	PPIA	CD38	MYH10	LIFR
DNM2	S100A8	MGAM	MASP2	HMCN1	THY1	APOC3
VTN	GPX3	PROM1	LDHA	PSMA7	ENTPD2	S100A9
GSTP1	C1R	LRG1	ALDOA	YWHAZ	UBE2D3	HPX
ENO1	AGRN	TNXB	HSPA1B	SELENOP	ATP5F1A	APRT
CAPN1	NEU1	TPI1	GSTA2	HSP90AB1	DBI	IL6ST
NAMPT	APOD	RNASE3	SI	PRDX6	WWP2	LBP
CA1	FCGR3A	F12	PRKACA	ENO3	ACTA1	COL6A1
CRYAB	EPHX2	PLSCR1	CANT1	SAA4	HRG	NPR3
FCGR3B	H2AX	A2M	GSTT1	DDAH2	ACTN4	GC
CD59	CPB2	DDAH1	IGFBP7	FASN	LAP3	ANXA7
DES	IRAK1	CEACAM1	COL6A3	CFB	GSTM3	AMBP
DPP4	EEF2	GOT1	CLEC3B	UMOD	VPS28	SERPING1
PTPA	TOLLIP	LGALS1	LAMC1	SFN	FSTL1	PRDX2
B2M	CUBN	PRDX5	LAMB2	CEACAM5	CBR1	ITCH
TGM2	ANXA2	SAA1	FABP4	PEPD	SELENBP1	SLC3A2
ANXA1	IQGAP1	VDAC1	THBS4	DEFA1	ART3	

Table 7
Gene name reported in PubMed.

IL6	IL1B	MPO
SOD1	MMP9	CAT

right, and is also a small amount of protein in the upper and lower left could be seen.

3.7. Core gene recognition

After PPI protein was analyzed by 252 unreported intersection genes, and protein interaction table was derived, ten Hub genes were screened out according to Degree value in Cytoscape, in which CD44, ACTB, FN1,ITGB1, PLG, CASP3, ALB, HSP90AA1, EGF, GAPDH were noticed (Fig. 9)

3.8. qRT-PCR findings

We used qRT-PCR to evaluate the effect of husc in CIR improvement. The results showed that the mRNA expression of ACTB, ALB, CASP3, CD44, ITGB1, FN1, PLG and GAPDH were higher in the CIR group than in the sham group. Comparing after the treatment of husc, the mRNA expression of ACTB, ALB, CASP3, CD44, ITGB1 and GAPDH were decreased related to the CIR group. Whereas, the mRNA expression of FN1 and PLG were higher in the hUSCs group than in the CIR group. Moreover, the mRNA expression level of EGF was decreased in the CIR group compared with that in the sham group, but upregulated in after the treatment of hUSCs, than that of the CIR group (Fig. 10).

Table 8
Genes unreported in PubMed.

No gene list was reported after query						
CST3	ENO2	TXN	PLAU	ABCB1	GOT2	CDC42
F2	ACTA2	CP	SMPD1	MUC1	TF	LTF
ACE	SERPINA3	EGF	HP	SERPINA1	C4A	ITGAV
ENG	KNG1	IDH1	MME	CKB	ACTC1	EPX
CASP3	SERPINI1	APOA1	THBS1	COMT	SERPINF2	FABP1
EDN1	CXCL12	HSPB1	HSPG2	BGN	LRP2	PRDX1
SERPINC1	GP1BA	PROCR	RPS27A	GLO1	FASLG	GGT1
COL4A2	GSR	PSAP	GAPDH	SOD3	CTSG	SERPINA4
SOD2	CD36	FGA	VCP	AQP1	NT5E	CD55
MIR21	CASP9	CLU	GSS	PROS1	HSP90AA1	SERPINF1
ALB	PON1	CTSD	ACTB	PLA2G2A	GDF15	TKT
MB	PLG	FGB	FN1	COL18A1	RETN	NID1
MMP2	APOH	HSPA8	MIF	AKR1B1	LGALS3	AHSG
ELANE	AGT	MIR146A	ITGB1	RAC1	ACE2	PTGDS
AOC1	FGF2	PPARG	TERT	LCN2	NAXE	GNA11
S100A9	APOB	TIMP1	FABP3	C3	PNP	CD14
IL6ST	HSPA1A	FLNA	CTSL	NAGLU	SLC9A3R2	CHI3L1
NPR3	G6PD	ANXA5	PARK7	CASP8	ACP1	C5
AMBP	VCAM1	ITGAM	SPP1	CFH	KL	ALDH9A1
CR1	CTSB	ACTG1	IGFBP2	CD44	MYH10	TGM2
KRT18	GUSB	AXL	PPIA	CD38	THY1	ANXA1
DNM2	S100A8	MGAM	MASP2	HMCN1	ENTPD2	LIFR
VTN	GPX3	PROM1	LDHA	PSMA7	UBE2D3	APOC3
GSTP1	C1R	LRG1	ALDOA	YWHAZ	ATP5F1A	ANXA2
ENO1	AGRN	TNXB	HSPA1B	SELENOP	DBI	IQGAP1
CAPN1	NEU1	TPI1	GSTA2	HSP90AB1	WWP2	HPX
NAMPT	APOD	RNASE3	SI	PRDX6	ACTA1	APRT
CA1	FCGR3A	F12	PRKACA	ENO3	HRG	SAA1
CRYAB	EPHX2	PLSCR1	CANT1	SAA4	ACTN4	VDAC1
FCGR3B	H2AX	A2M	GSTT1	DDAH2	LAP3	LBP
CD59	CPB2	DDAH1	IGFBP7	FASN	GSTM3	COL6A1
DES	IRAK1	CEACAM1	COL6A3	CFB	VPS28	FABP4
DPP4	EEF2	GOT1	CLEC3B	UMOD	FSTL1	THBS4
PTPA	TOLLIP	LGALS1	LAMC1	SFN	CBR1	GC
B2M	CUBN	PRDX5	LAMB2	CEACAM5	SELENBP1	ANXA7
SLC3A2	PRDX2	SERPING1	ITCH	DEFA1	ART3	PEPD

4. Discussion

We conducted animal experiments to verify that husc can improve the neural function in CIR rats, and analyzed the gene network changes after CIR treated with cells transplantation, combined with bioinformatics. We looking for cross-genes from Genecars [16]. Combined with Venny analysis, and integrated reported and unreported genes in PubMed and CNKI. 252 key genes unreported we performed protein interaction of GO, KEGG and PPI. According to GO enrichment [17], neutrophil degranulation is crucial in BP, vesicle Lumen is an important process of cell composition. Neutrophil degranulation is modulated by cell transplantation during cerebral ischemia. In addition, neutrophil degranulation and neutrophil activation involved in immune response are the terms with the largest number of BP enrichment in our analysis, and enzyme activity is the term with the largest number of MF rich sets. From KEGG pathway analysis, we can see that complement and coagulation cascades is the most important pathway. Importantly, hub gene included CD44, ACTB, FN1, ITGB1, PLG, CASP3, ALB, HSP90AA1, EGF, and GAPDH, was confirmed by q-PCR.

4.1. Neurological improvement after husc treatment

As husc can be obtained in a non-invasive way (Bento, Shafigullina et al., 2020), it has a potential for the treatment of CIR. In this study, we found that husc transplanted into the lateral ventricle can improve the neurological function in husc treated group at day 14. Literaturely, Liang reported that exosomes from husc enhanced cell proliferation and neuronal differentiation via miR-26a/HDAC6 axis in vitro neural stem cells model of ischemic stroke which were treated with oxygen-glucose deprivation/reoxygenation [18]. Wu found that transplantation of neural progenitor cells induced from husc can significantly improve neurological functions with migration of cells from the grafted side to the lesion side in stroke rats undergoing transient middle cerebral artery occlusion (tMCAO) reperfusion [19]. Zhang reported that MicroRNA-216a-5p from exosomes secreted by husc ameliorate ischemia/reperfusion injury through decreasing PTEN levels and stimulating Akt phosphorylation in HK-2 cells [20]. In addition, the beneficial potential of husc can be improved by genetic modifications has been reported, suggesting husc can be considered as a cell vector that could help gene therapy (Salehi, MS,. et al. (2022). Tegother, the effect of husc in improving neurological function after brain ischemia is certain in these observations. **Gene network and its functional implication**.

With the rapid development of modern medicine, stem cell transplantation is considered to have great potential in treating
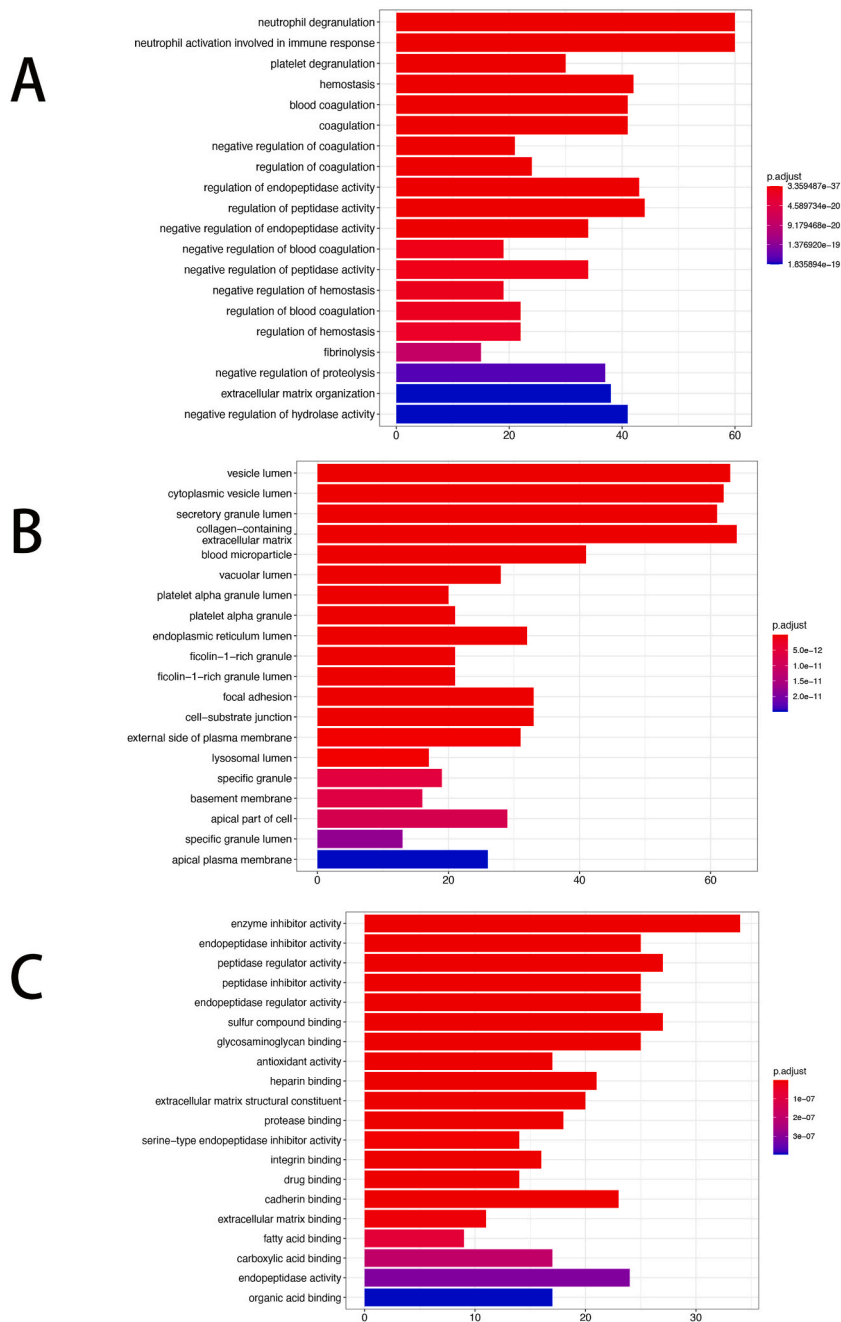
Fig. 6. Enrichment diagram of GO analysis. A. Biological processes (BP), B. Cellular components (CC) and C are involved in enrichment analysis. Top 20 factors of molecular function (MF).

neurological diseases, including stroke. Literature has found that MSC can treat cerebral ischemia and prevent inflammation of glial cells induced by cerebral ischemia by inhibiting TLR4 [21]. Compared to other stem cells, husc possess several [22]. The collection method from human urine is simple, non-invasive, reproducible and acceptable, and avoids the ethical issues raised by the use of other tissues. Though there has report in husc promoting stroke recovery [23], the molecular network mechanism of husc therapy for stroke is unclear. This paper is the first report and show the molecular network mechanism of husc in CIR, according to gene network relationship [24].
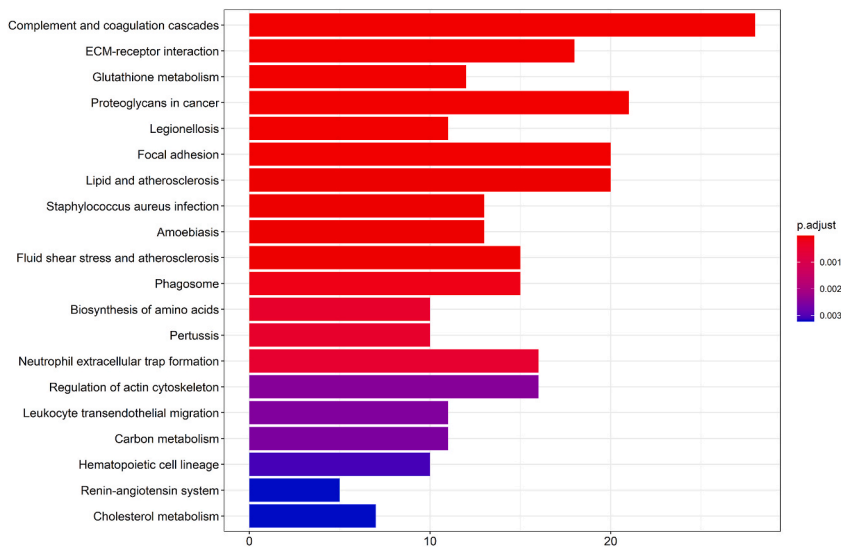
Fig. 7. Analysis of KEGG pathway.
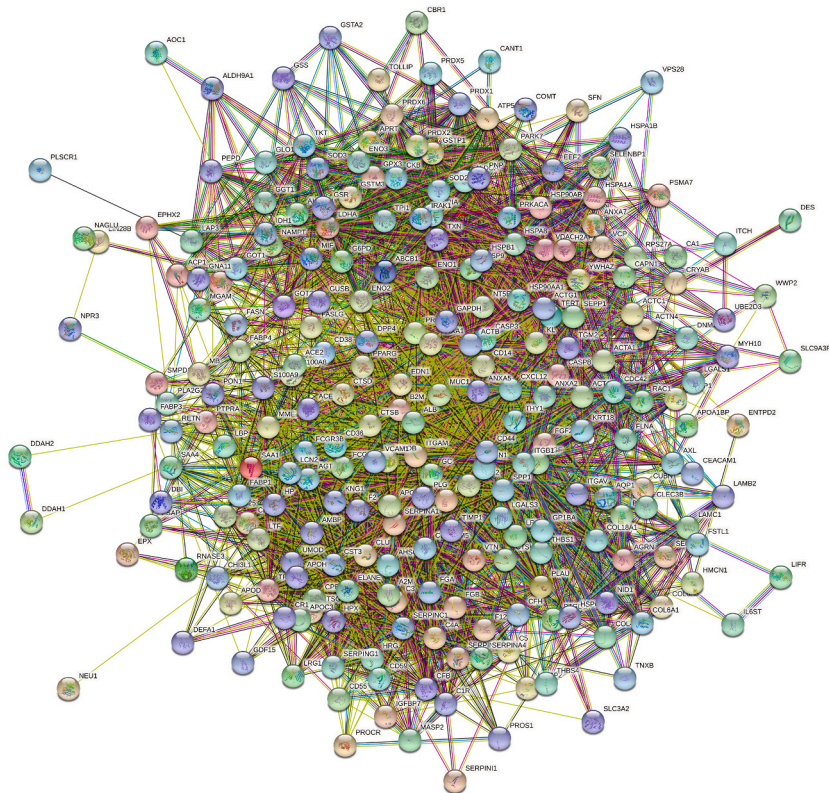
Fig. 8. PPI network of genes interaction.

4.2. Were integrated unreported genes to get core genes

So far, the commonly used strategy of bioinformatics is to query targets in the database. Due to the timeliness of genes, previous research summaries reported, but the latest PubMed literature results are not included. Therefore, we specially supplemented the latest literature results related to husc. Compared with the results of intersection, 252 intersecting genes that had never been reported in literature. This therefore provides important gene network for stem cell therapy by different data integration. **Implication of GO**
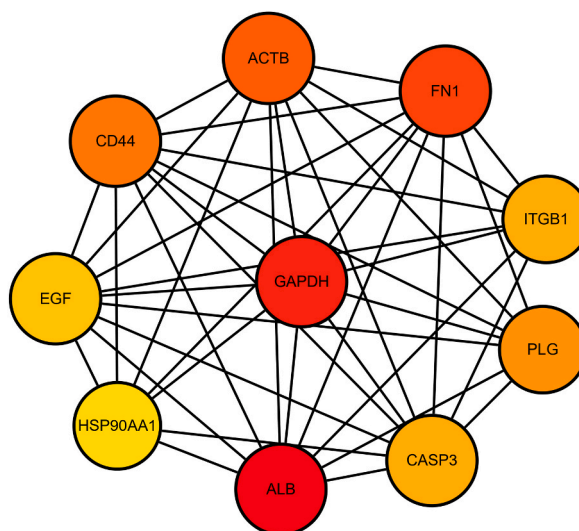
Fig. 9. The Hub genes.
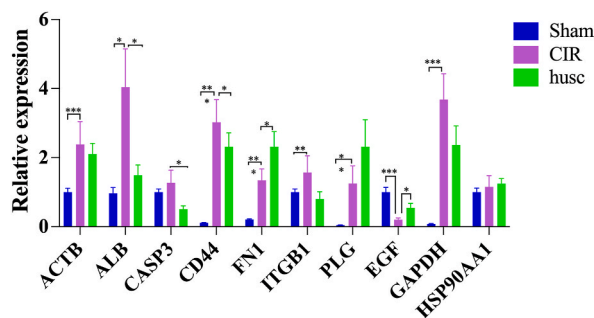
Fig. 10. The relative mRNA expression of CD44, ACTB, FN1, ITGB1, PLG, CASP3, ALB, HSP90AA1, EGF and GAPDH in the sham, CIR and husc group.

enrichment and KEGG pathway analysis.

GO enrichment analysis showed that neutrophil degranulation was crucial in BP. Neutrophils can become inflammatory and infected [25]. According to the literature, after CIR, neutrophils will accumulate in the pia meningeal and perivascular space, and eventually reach the infarcted brain parenchyma [26]. In the co-expression module, the lumen is an important process of cell composition. Endodermal vesicles are the best spatial and temporal indexes [27]. In addition, enzyme inhibitor activity was the term with the largest number of MF concentrations in our analysis [28]. Activity of enzyme inhibitors may alleviate neuronal damage caused by ischemic stroke [29].

KEGG pathway analysis showed that the treatment of CIR by husc involved the first ten signaling pathways: included Complement and coagulation cascades, ECM-receptor interaction, Glutathione metabolism, Proteoglycans in cancer, Legionellosis, Focal adhesion, Lipid and atherosclerosis, Staphylococcus aureus infection, Amoebiasis, Fluid shear stress and atherosclerosis [30]. The metabolic network we constructed will help to select molecular targets and elucidate the molecular mechanisms of cerebral ischemia [31]. Complement and coagulation cascade are the most important pathways in KEGG. When adjust is the highest, Count is the highest, therefore differential expression is the most significant. It is believed to be closely related to the treatment of CIR by huscl transplantation and may be involved in its occurrence and progression [32]. In complement and coagulation cascade signaling, coagulation cascade is used to target proteolysis on the surface of activated platelets. If platelets are activated by exposure to an activated endothelium, they are released to promote the formation of microvesicles that bind to platelet adhesion mediators, clotting factors, and adjacent receptors on the membrane, hydrolysis of the proenzyme cascade proteins into active enzymes, and thrombin production [33]. The occurrence of coagulation cascade may promote cerebral ischemia through thrombin [30]. In the ECM-receptor interaction signaling pathway, ECM-receptor interaction may promote the formation of husc. In glutathione metabolic signaling pathways, glutathione can be exported and imported through the plasma membrane of many cells [34]. Glutathione metabolism plays a role in shaping the immune microenvironment [35]. Among the proteoglycan signaling pathways in cancer, proteoglycan inhibits effectively tumor growth in cancer [36]，In the Legionnaires' disease signaling pathway, legionnaires' disease may be a pathogen produced after husc transplantation [37]. An important step in cell migration is adhesion to the substrate with specific adhesion points in the adhesion

spot signaling pathway [38]. In the lipid and atherosclerotic signaling pathways, atherosclerosis, as a chronic inflammation of the artery wall, is widespread, which is presenting damage and plaque accumulation in the intima of the artery wall. At the same time, plaque erosion and rupture can lead to blood clots, and atherosclerosis may develop in the brain after their cells are transplanted [39].

Staphylococcus aureus infections in the signal path, staphylococcus aureus, as a kind of symbiotic organism infection, may be accompanied by anthropogenic urine infection occurs in the process, stem cell transplants in amoebiasis signaling pathways, amoebiasis was dissolved in the organization amoebic caused in the gut of native animal diseases, the anthropogenic urine amoebiasis disease may occur after stem cell transplantation. Fluid shear stress induces apoptosis of husc in both fluid shear stress and atherosclerotic signaling pathways, and atherosclerosis may lead to thrombosis in cerebral ischemia [40].

4.3. Protein interaction and its significance

This paper analyzes the network interaction between CIR and various proteins expressed in husc [41,42]. As you can see, there are a lot of histones, mainly in a round cluster of proteins in the middle. Secondly, there is a protein relationship formed at the upper right, including a small amount of protein in the upper and lower left. Among them, CPB2, APOH, MIF, CTSG, TIMP1, MMP2, VTN, APOC3, GAPDH and HRG are the most important proteins [43]. Among the 10 most important proteins, there are close connections between each protein. In addition to the strong interaction between the above proteins, DDAH2 and DDAH1 in the lower left corner and IL6 ST in the lower right corner have direct interaction with LIFR. These proteins may indicate the stage of CIR interaction with husc, suggesting these molecular network interpretations play an important role in husc transplantation during cerebral ischemia reperfusion. Literature has shown that husc contribute to functional recovery of cerebral ischemia, and their molecules are regulated by mulfiple genes [44]. In this study, we reported the effect of huse in CIR and revealed the core gene network. Hub gene found mag include: CD44, ACTB, FN1, ITGB1, PLG, CASP3, ALB, HSP90AA1, EGF, GAPDH. We predict that these 10 genes have a regulatory role in CIR.

4.3.1. qRT-PCR validated the gene expression and its functional implication

In this study, we confirmed the multiple gene change in husc treated CIR. Of these, CD44, a transmembrane glycoprotein, known to be involved in regulation of cytokine gene expression, lymphocyte trafficking and endothelial cell recognition in inflammatory diseases, has been involved in our observation. Previously, it is has been reported that CD44 expression was inhibited when SD rats with cerebral ischemia-reperfusion injury were treated with Leonuri Herba Total Alkali [45]. This indirectly indicated that CD44 is up-regulated in CIR and may be involved in the occurrence and development of CIR. Similarly, Wang X et al. found that [46] the expression of CD44 mRNA was induced in a mouse model of cerebral ischemia.

Act-β has been recognized as the most stably expressed endogenous genes, [47]. Moreover, GAPDH, a glycolytic enzyme, was also used as the endogenous gene. However, Li C et al. pointed out that [48] GAPDH shared S-nitroylation, Siah1 binding, translocation to nucleus, and concomitant neuron death occur during the early stages of reperfusion in the rat four-vessel occlusion ischemic model. Similarly, over-expression of GAPDH in nucleus resulted in neuronal apoptosis induced by CIR [49]. Here, we showed the change of β-actin and GADPH after CIR with husc treatment may have some indicationssimilar to past finding of GADPH in CIR.

Fibronectin 1 (Fn1) was markedly elevated in the heart of I/R pigs and ischemic patients and inhibition of Fn1 may be a novel therapeutic option for treating ischemic heart diseases [50]. Nevertheless, there was no experimental research reported the role of Fn1 in CIR. Thus, we speculated Fn1 was upregulated in CIR with husc treatment condition, indicating this molecule mas been involved in our observation.

Integrin β1 played a key role in the repair and protection of neurovascular units by promoting angiogenesis In the process of CIR. The inhibition of Integrin β1 pathway during CIR aggravated the behavior and neurovascular regeneration of CIR rats [51]. These evidences indicated that Integrin β1 was downgraded in CIR. Our study reported the expression of integrin β1 was downregulated in CIR after husc treatment, supplying the novel evidence to understand the role of integrin β1 in CIR with husc treatment.

In clinical settings, tissue plasminogen activator (t-PA) for thrombolytic therapy is the most important thrombolytic drug of ischemic stroke and has neuroprotective effects [52]. Some research found that [53] tPA knocking out significantly aggravated brain injury and increased neuronal apoptosis and mitochondrial damage, which indicated that tPA may inhibit apoptosis and improve mitochondrial function. In addition, accumulating evidence has suggested that [54,55] apoptosis played an important role in the occurrence and development of CIR, corresponding to the increase of Caspase3. Whereas, Albumin (ALB), a potent antioxidant [56] had neuroprotective effects on cerebral hemorrhage, focal and global cerebral ischemia and subarachnoid hemorrhage [57]. In particular, ALB administration abated neuronal apoptosis after cerebral hemorrhage at least in part through the ERK/Nrf2/HO-1 signaling pathway [57]. Comparatively, literature report, we just found the expression of AIB and caspase-3 in CIR subjected to husc treatment, suggesting effect of husc in CIR may be derived the inhibition of these genes.

Oppositely, one study suggested that [58] epidermal growth factor (EGF) had protective effects on ischemic injury via activating EGF receptor (EGFR). Further, EGF/EGFR activation ameliorated infarct volume of brain tissues and neurological deficit. Moreover, Tang Y et al. pointed out that [59] EGF pretreatment significantly decreased neurological deficit and infarct volume. In addition, EGF pretreatment increased the expression of Bcl-2 and reduced the expression of Bax. These evidences indicated that EGF protect against apoptosis, neurological deficit and infarct in CIR.

Ma D et al. suggested that [60] HSP90AA1 might be related to the pathogenesis of I/R injury via weighted gene co-expression network analysis. However, the role of HSP90AA1 in CIR-induced injury is not well illustrated. In our study, we reported EGF decreased after CIR but reversed in husc administered condition, indicating EGF is a crucial molecule in CIR with husc addition, which is largely different form the HSP90AA1, with no change in this study.

5. Conclusion

It can conclude that husc transplantation improve effectively neural behavior in CIR rats, and the underlying mechanism is involving multiple genes, in which, ALB, caspase-3, CD44, ITGB1, even ACTB, and GADPH was significantly increased in CIR and decreased in husc treatment. All of these findings could provide novel evidences in molecular network to understand the effect of husc in CIR treatment.

Ethical approval

All procedures were performed in accordance with the guidelines and approval of the Ethics Committee of the Kunming Medical University, and approved by the Animal Experiment Ethics Committee of Kunming Medical University, with number KMMU20220891.

Human and animal ethics

The Ethical approval number for the husc extraction, is YLS2021-55, white the animal ethics code is KMMU20220891.

Public consent

I declared that all authors agree to publish.

Whether there is supporting data

I declared that the data and materials contained in this manuscript have not been published elsewhere and are available.

Raw data declaration

I declare that all original data are contained in this manuscript and attached materials without reservation, and that the data and materials contained in this manuscript have not been published elsewhere.

CRediT authorship contribution statement

Lang-Chun Zhang: Writing – review & editing, Writing – original draft. **Na Li:** Methodology, Data curation. **Ji-Lin Chen:** Data curation. **Jie Sun:** Resources. **Min Xu:** Data curation. **Wen-Qiang Liu:** Data curation. **Zhong-Fu Zuo:** Data curation. **Lan-Lan Shi:** Data curation, Conceptualization. **Ting-Hua Wang:** Visualization, Funding acquisition. **Xiang-Yin Luo:** Writing – review & editing, Methodology.

Declaration of competing interest

The authors declare that they have no known competing financial interests or personal relationships that could have appeared to influence the work reported in this paper.

Acknowledgement

References

[1] P. Guo, et al., Effects of irisin on the dysfunction of blood-brain barrier in rats after focal cerebral ischemia/reperfusion, Brain Behav 9 (10) (2019) e01425.
[2] Z. Shen, et al., PARK2-dependent mitophagy induced by acidic postconditioning protects against focal cerebral ischemia and extends the reperfusion window, Autophagy 13 (3) (2017) 473–485.
[3] S. Li, et al., Dental pulp stem cell-derived exosomes alleviate cerebral ischaemia-reperfusion injury through suppressing inflammatory response, Cell Prolif. 54 (8) (2021) e13093.
[4] T.R. Doeppner, D.M. Hermann, Mesenchymal stem cells in the treatment of ischemic stroke: progress and possibilities, Stem Cells Cloning 3 (2010) 157–163.
[5] Y. Huang, et al., CUEDC2 ablation enhances the efficacy of mesenchymal stem cells in ameliorating cerebral ischemia/reperfusion insult, Aging (Albany NY) 13 (3) (2021) 4335–4356.
[6] A.C. Boese, et al., Neural stem cell therapy for subacute and chronic ischemic stroke, Stem Cell Res. Ther. 9 (1) (2018) 154.
[7] J.Y. Choi, et al., Potency of human urine-derived stem cells for renal lineage differentiation, Tissue Eng Regen Med 14 (6) (2017) 775–785.
[8] T. Zhou, et al., Generation of human induced pluripotent stem cells from urine samples, Nat. Protoc. 7 (12) (2012) 2080–2089.
[9] X. Ji, et al., Urine-derived stem cells: the present and the future, Stem Cells Int 2017 (2017) 4378947.
[10] R. Wu, et al., Functional characterization of the immunomodulatory properties of human urine-derived stem cells, Transl. Androl. Urol. 10 (9) (2021) 3566–3578.
[11] Y. Hwang, et al., Direct differentiation of insulin-producing cells from human urine-derived stem cells, Int. J. Med. Sci. 16 (12) (2019) 1668–1676.

[12] Y.Z. Huang, et al., Urine-Derived Stem Cells for Regenerative Medicine: Basic Biology, Applications, and Challenges, Tissue Eng Part B Rev, 2022.

[13] C. Wang, et al., RNA-seq based transcriptome analysis of endothelial differentiation of bone marrow mesenchymal stem cells, Eur. J. Vasc. Endovasc. Surg. 59 (5) (2020) 834–842.

[14] Y.F. Zhang, et al., Systematic elucidation of the mechanism of geraniol via network pharmacology, Drug Des. Dev. Ther. 13 (2019) 1069–1075.

[15] R. Zhang, et al., Salt-inducible kinase 2 regulates energy metabolism in rats with cerebral ischemia-reperfusion, Zhejiang Da Xue Xue Bao Yi Xue Ban 50 (3) (2021) 352–360.

[16] M. Safran, et al., GeneCards Version 3: the Human Gene Integrator vol. 2010, Database, Oxford, 2010, p. baq020.

[17] H. Wang, H. Zheng, D.Z. Chen, TANGO: A GO-Term Embedding Based Method for Protein Semantic Similarity Prediction, IEEE/ACM Trans Comput Biol Bioinform, 2022.

[18] X. Ling, et al., Exosomes from human urine-derived stem cells enhanced neurogenesis via miR-26a/HDAC6 axis after ischaemic stroke, J. Cell Mol. Med. 24 (1) (2020) 640–654.

[19] R. Wu, et al., Transplantation of neural progenitor cells generated from human urine epithelial cell-derived induced pluripotent stem cells improves neurological functions in rats with stroke, Discov. Med. 29 (156) (2020) 53–64.

[20] Y. Zhang, et al., Transfer of MicroRNA-216a-5p from exosomes secreted by human urine-derived stem cells reduces renal ischemia/reperfusion injury, Front. Cell Dev. Biol. 8 (2020) 610587.

[21] G. Cai, et al., Mesenchymal stem cell-derived exosome miR-542-3p suppresses inflammation and prevents cerebral infarction, Stem Cell Res. Ther. 12 (1) (2021) 2.

[22] N. Pavathuparambil Abdul Manaph, et al., Urine-derived cells for human cell therapy, Stem Cell Res. Ther. 9 (1) (2018) 189.

[23] B. Artegiani, et al., A single-cell RNA sequencing study reveals cellular and molecular dynamics of the hippocampal neurogenic niche, Cell Rep. 21 (11) (2017) 3271–3284.

[24] S. Fishilevich, et al., GeneHancer: Genome-wide Integration of Enhancers and Target Genes in GeneCards vol. 2017, Database, Oxford, 2017.

[25] F. Mollinedo, Neutrophil degranulation, plasticity, and cancer metastasis, Trends Immunol. 40 (3) (2019) 228–242.

[26] A. Otxoa-de-Amezaga, et al., Location of neutrophils in different compartments of the damaged mouse brain after severe ischemia/reperfusion, Stroke 50 (6) (2019) 1548–1557.

[27] M.J. Haley, C.B. Lawrence, The blood-brain barrier after stroke: structural studies and the role of transcytotic vesicles, J. Cerebr. Blood Flow Metabol. 37 (2) (2017) 456–470.

[28] H. Alatan, et al., Extracellular matrix-related hubs genes have adverse effects on gastric adenocarcinoma prognosis based on bioinformatics analysis, Genes 12 (7) (2021).

[29] J.W. Min, et al., USP14 inhibitor attenuates cerebral ischemia/reperfusion-induced neuronal injury in mice, J. Neurochem. 140 (5) (2017) 826–833.

[30] Y. Xie, et al., Revealing the mechanism of astragali radix against cancer-related fatigue by network pharmacology and molecular docking, Evid Based Complement Alternat Med 2021 (2021) 7075920.

[31] M. Liu, et al., An evidence-based review of related metabolites and metabolic network research on cerebral ischemia, Oxid. Med. Cell. Longev. 2016 (2016) 9162074.

[32] X. Fang, et al., Enrichment analysis of differentially expressed genes in chronic heart failure, Ann. Palliat. Med. 10 (8) (2021) 9049–9056.

[33] D. Green, Coagulation cascade, Hemodial. Int. 10 (Suppl 2) (2006) S2–S4.

[34] J. Oestreicher, B. Morgan, Glutathione: subcellular distribution and membrane transport (1), Biochem. Cell. Biol. 97 (3) (2019) 270–289.

[35] Y. Xiao, D. Meierhofer, Glutathione metabolism in renal cell carcinoma progression and implications for therapies, Int. J. Mol. Sci. 20 (15) (2019).

[36] J. Wei, et al., Roles of proteoglycans and glycosaminoglycans in cancer development and progression, Int. J. Mol. Sci. 21 (17) (2020).

[37] M. Mikulska, et al., Legionellosis after hematopoietic stem cell transplantation, Bone Marrow Transplant. 56 (10) (2021) 2555–2566.

[38] E.K. Paluch, I.M. Aspalter, M. Sixt, Focal adhesion-independent cell migration, Annu. Rev. Cell Dev. Biol. 32 (2016) 469–490.

[39] A. Poznyak, et al., The diabetes mellitus-atherosclerosis connection: the role of lipid and glucose metabolism and chronic inflammation, Int. J. Mol. Sci. 21 (5) (2020).

[40] K. Rennier, J.Y. Ji, The role of death-associated protein kinase (DAPK) in endothelial apoptosis under fluid shear stress, Life Sci. 93 (5–6) (2013) 194–200.

[41] J. Zhou, et al., Protein function prediction based on PPI networks: network reconstruction vs edge enrichment, Front. Genet. 12 (2021) 758131.

[42] D. Vella, et al., MTGO: PPI network analysis via topological and functional module identification, Sci. Rep. 8 (1) (2018) 5499.

[43] W.Q. He, et al., The PPI network and clusters analysis in glioblastoma, Eur. Rev. Med. Pharmacol. Sci. 19 (24) (2015) 4784–4790.

[44] W. Pan, et al., Human urine-derived stem cell-derived exosomal miR-21-5p promotes neurogenesis to attenuate Rett syndrome via the EPha4/TEK axis, Lab. Invest. 101 (7) (2021) 824–836.

[45] Y. Li, et al., Protection against acute cerebral ischemia/reperfusion injury by Leonuri Herba Total Alkali via modulation of BDNF-TrKB-PI3K/Akt signaling pathway in rats, Biomed. Pharmacother. 133 (2021) 111021.

[46] X. Wang, et al., CD44 deficiency in mice protects brain from cerebral ischemia injury, J. Neurochem. 83 (5) (2002) 1172–1179.

[47] P.E.L. Day, et al., Validation of control genes and a standardised protocol for quantifying gene expression in the livers of C57BL/6 and ApoE-/- mice, Sci. Rep. 8 (1) (2018) 8081.

[48] C. Li, et al., Cerebral ischemia-reperfusion induces GAPDH S-nitrosylation and nuclear translocation, Biochemistry (Mosc.) 77 (6) (2012) 671–678.

[49] Y.Z. Guan, et al., [Involvement of inhibition of nucleus GAPDH over-expression in erythropoietin's reduction of neuronal apoptosis induced by brain ischemia/reperfusion in rats], Sheng Li Xue Bao 64 (3) (2012) 269–274.

[50] Y.L. Zhang, et al., Blockage of fibronectin 1 ameliorates myocardial ischemia/reperfusion injury in association with activation of AMP-LKB1-AMPK signaling pathway, Oxid. Med. Cell. Longev. 2022 (2022) 6196173.

[51] X.L. Li, et al., Effects of Integrin β1 on behavior and neurovascular regeneration in rats with cerebral ischemia-reperfusion injury, Eur. Rev. Med. Pharmacol. Sci. 23 (8) (2019) 3487–3494.

[52] T. Fukuta, et al., Applications of liposomal drug delivery systems to develop neuroprotective agents for the treatment of ischemic stroke, Biol. Pharm. Bull. 42 (3) (2019) 319–326.

[53] Y. Cai, et al., FUNDC1-dependent mitophagy induced by tPA protects neurons against cerebral ischemia-reperfusion injury, Redox Biol. 38 (2021) 101792.

[54] Z.Q. Shao, et al., Apelin-13 inhibits apoptosis and excessive autophagy in cerebral ischemia/reperfusion injury, Neural Regen Res 16 (6) (2021) 1044–1051.

[55] L. Gong, et al., RTN1-C mediates cerebral ischemia/reperfusion injury via ER stress and mitochondria-associated apoptosis pathways, Cell Death Dis. 8 (10) (2017) e3080.

[56] M. Pinsky, et al., Human serum Albumin facilitates heme-iron utilization by fungi, mBio 11 (2) (2020).

[57] L. Belayev, et al., Albumin treatment reduces neurological deficit and protects blood-brain barrier integrity after acute intracortical hematoma in the rat, Stroke 36 (2) (2005) 326–331.

[58] D.H. Peng, et al., Epidermal growth factor alleviates cerebral ischemia-induced brain injury by regulating expression of neutrophil gelatinase-associated lipocalin, Biochem. Biophys. Res. Commun. 524 (4) (2020) 963–969.

[59] Y. Tang, et al., JAK2/STAT3 pathway is involved in the neffects of epidermal growth factor receptor activation against cerebral ischemia/reperfusion injury in rats, Neurosci. Lett. 662 (2018) 219–226.

[60] D. Ma, et al., Weighted gene co-expression network analysis to investigate the key genes implicated in global brain ischemia/reperfusion injury in rats, Adv. Clin. Exp. Med. 29 (6) (2020) 649–659.